OncoTargets and Therapy

Dovepress
open access to scientific and medical research

Open Access Full Text Article

ORIGINAL RESEARCH

AKT2-knockdown suppressed viability with enhanced apoptosis, and attenuated chemoresistance to temozolomide of human glioblastoma cells in vitro and in vivo

This article was published in the following Dove Press journal:
OncoTargets and Therapy
8 July 2015
Number of times this article has been viewed

Yong Cui[1,*]
Jing Lin[1,*]
Jianling Zuo[2]
Lei Zhang[1]
Yan Dong[1]
Guohan Hu[1]
Chun Luo[1]
Juxiang Chen[1]
Yicheng Lu[1]

[1]Department of Neurosurgery, Changzheng Hospital, Second Military Medical University, Shanghai, People's Republic of China; [2]Department of Neurosurgery, First Affiliated Hospital of Soochow University, Suzhou, People's Republic of China

*These authors contributed equally to this work

Abstract: The AKT2 kinase (protein kinase Bβ) is overexpressed in high-grade gliomas. Upregulation of the *AKT2* gene has been previously observed in glioblastoma patients suffering from chemotherapy failure and tumor progress. In this study, we aimed to evaluate the effect of *AKT2* on viability and chemoresistance in the human glioblastoma cell line U251. The U251 cell line was stably transfected with short hairpin RNA (shRNA) targeting *AKT2*. U251 cells underexpressing *AKT2* were then examined for viability with temozolomide (TMZ) treatment, and tested for cell apoptosis both in vitro and in tumor-implanted mice. Next, expressions of several chemoresistance-related molecules were measured by quantitative reverse-transcription polymerase chain reaction (qRT-PCR) and western blot analysis. The results showed that the 50% inhibitory concentration (IC_{50}) of AKT2 shRNA-transfected cells was significantly lower compared with Lenti-GFP-transfected and nontransfected controls and that the tumor growth of the AKT2-shRNA and TMZ combined-treated mice was obviously suppressed in either mass or volume. Concomitantly, the apoptosis of TMZ-treated tumor cells was significantly enhanced after knockdown of *AKT2*, as measured by flow cytometry and in situ terminal deoxynucleotidyl transferase dUTP nick end labeling (TUNEL) analysis. Furthermore, *AKT2*-inhibition in TMZ-treated glioblastoma U251 cells upregulated apoptotic effector caspase-3, whereas it downregulated antiapoptotic protein Bcl-2, DNA repairing protein MGMT, and drug efflux pump protein MRP1. Our study identified *AKT2* as an important gene in presenting chemoresistance in glioblastoma, and a potential target to potentiate the clinical effect of chemotherapy in glioma treatment.

Keywords: AKT2, glioma, chemoresistance, TMZ, mice

Introduction

Glioblastoma multiforme (GBM), also known as grade IV astrocytoma, is the most frequent primary neoplasms of the central nervous system in adults, accounting for 52% of all functional tissue brain tumor cases and 20% of all intracranial tumors. Even with intensive intervention incorporating surgery, chemotherapy, and radiotherapy, the prognosis for GBM patients remains poor: tumors invariably recur, and survival beyond 2 years is less than 20%.[1,2]

AKT2 is a member of the serine/threonine kinase family.[3] It is involved in the PI3K/AKT pathway and has been linked to cell proliferation, invasiveness, metastasis, angiogenesis, and drug resistance in a variety of human cancers, including pancreatic, prostate, ovarian, thyroid, and breast cancers.[4–10] Our previous research also indicated that downregulation of AKT2 in the glioblastoma cell line U87 inhibited proliferation,

Correspondence: Yicheng Lu
Department of Neurosurgery, Changzheng Hospital, Second Military Medical University, 415 Fengyang Road, Shanghai 200003, People's Republic of China
Tel +86 21 5423 7166
Fax +86 21 5423 7166
Email jlin.ldr@gmail.com

induced apoptosis, and enhanced the chemosensitivity to teniposide (VM-26). More fundamentally, we found that *AKT2* gene expression was higher in gliomas of more advanced pathological stage, and revealed *AKT2* expression as an independent negatively prognostic indicator of patient survival time. Moreover, our gene chip-based analysis revealed that *AKT2* was one of the significantly overexpressed genes that affected the survival duration of glioblastoma patients receiving same antineoplastic drug semustine.[11,12] Based upon these findings, we proposed the hypothesis that *AKT2* can play an important role in regulating glioma cell chemoresistance in addition to its role in tumorigenicity.

In a recent clinical trial, temozolomide (TMZ) demonstrated modest activity against recurrent glioma, and its combination with radiotherapy significantly prolonged survival of newly diagnosed patients.[13] Thus, TMZ combined with radiotherapy became the standard of care for GBM treatment.[14] However, the average survival with TMZ standard treatment is only 14–16 months, which highlights a fundamental hallmark of GBM chemoresistance, specifically, multidrug resistance (MDR). The mechanisms of MDR are complex and multifactorial, and could be conferred by a broad spectrum of molecular processes involved in different regulating pathways. For instance, the acquisition of MDR phenotype has been closely associated with drug transporters, drug-induced apoptosis, and DNA repair genes.[15,16]

Generally speaking, we hereby tested our hypothesis to evaluate the effect of *AKT2* on viability and chemoresistance in the human glioblastoma cell line U251, aiming to demonstrate the role of *AKT2* in multiple chemoresistance-related pathways, as a potential target for overcoming chemoresistance.

Materials and methods

Cell culture

The human glioblastoma cell line U251 was purchased from the Chinese Academy of Sciences (Shanghai, People's Republic of China). All cell lines, including the parental glioblastoma cell line and the modified lines described below, were grown in Dulbecco's Modified Eagle's Medium (DMEM) supplemented with 10% fetal bovine serum (FBS), 100 U/mL penicillin G, 100 mg/mL streptomycin, and 1.5 mM L-glutamine. Cells were maintained in monolayer culture at 37°C, in humidified air with 5% CO_2.

Constructs and transfection

Four different short hairpin RNA (shRNA) sequences were constructed into LV3 vectors and then tested for inhibitory activity by transient transfection into 293FT cells. The templates of shRNA for *AKT2* and control shRNA were designed with the loop structure TTCAAGAGA (Designer3.0; Genepharma, Shanghai, People's Republic of China). The most effective sequence specific for *AKT2* (5′-UGCCCUUCUACAACCAGGAdTdT-3′), as well as a control shRNA tagged with green fluorescent protein (GFP) (5′-UGCCGUUCUUCAACGAGGAdTdT-3′) were then inserted into the BamHI/EcoRI restriction sites of LV3, to make complete vectors, named AKT2-shRNA and Lenti-GFP. After transfection to 293FT cells, packed lentiviruses were harvested and then stably transfected to U251 cells in the presence of 5 μg/mL polybrene. After 2–3 weeks, single independent clones were randomly isolated and plated separately to be tested for *AKT2* RNA and protein expression. In this way, three U251 lines were established, one expressing an *AKT2*-specific shRNA, leading to stable underexpression of AKT2; another expressing GFP as negative control; and a U251 noninfected line, acting as blank control.

Protein extraction and western blotting

Cells from each experimental group were harvested and incubated with lysis buffer (100 μL) on ice for 30 minutes and then centrifuged at 12,000 rpm for 2 minutes at 4°C. The protein extract was detected using a bicinchoninic acid protein assay. A 20 μL protein sample was loaded onto polyacrylamide–sodium dodecyl sulfate (SDS) gels, separated by electrophoresis, and then transferred to nitrocellulose membranes. After blocking with 5% nonfat milk in phosphate-buffered saline with Tween® (PBST) for 1 hour at room temperature (RT), the membranes were blotted with primary antibody at 4°C overnight, followed by incubation with a peroxidase-conjugated secondary antibody (1:2,000; Jackson ImmunoResearch Laboratories Inc., West Grove, PA, USA) for 2 hours at 37°C. Bands on the membranes were visualized using enhanced chemiluminescence (Bio-Rad Laboratories, Hercules, CA, USA). The primary antibodies used were mouse monoclonal antibody to AKT2 (1:1,000; Abgent, San Diego, CA, USA), mouse monoclonal antibody to Bcl-2 (1:1,000; Santa Cruz Biotechnology Inc, Dallas, TX, USA), goat polyclonal antibody to caspase-3 (cleaved, active form, 1:1,000; Santa Cruz Biotechnology Inc), mouse monoclonal antibody to MDR1 (1:1,000; Santa Cruz Biotechnology Inc), goat polyclonal antibody to MRP1 (1:1,000; Santa Cruz Biotechnology Inc), and mouse monoclonal antibody to MGMT (1:1,000; PTG). A mouse antibody to GAPDH (1:1,000, Santa Cruz Biotechnology Inc) was used

as the internal control. Each western blotting procedure was performed in triplicate.

Quantitative reverse-transcription polymerase chain reaction (qRT-PCR) analysis

Total RNAs were extracted either from the three experimental cell lines or from frozen tissue samples for the in vivo experiment, using a RNeasy® mini kit (Qiagen, Venlo, the Netherlands). First-strand complementary DNA (cDNA) was reverse-transcribed from 1 μg total RNA using the SuperScript® First-Strand cDNA system (Invitrogen; Life Technologies Corp, Carlsbad, CA, USA) and amplified by Platinum® SYBR® Green qPCR SuperMix-UDG (Invitrogen; Life Technologies Corp). For each polymerase chain reaction (PCR) reaction, a master mix was prepared that included Platinum SYBR Green qPCR SuperMix-UDG, forward primer, reverse primer, and 10 ng template cDNA. GAPDH was used as internal control (Table 1).

Cell-inhibition ratio and TMZ-sensitivity assay

Cell growth was determined with a Cell Counting Kit-8 (CCK-8) colorimetric assay. AKT2-shRNA, Lenti-GFP, and the untransfected groups were replated onto 96-well plates at 5×10^5 cells/well in culture medium and left overnight to allow adherence. The medium was then replaced with fresh medium containing (or not) increasing concentrations of drug (1–128 μg/mL). After 72 hours, the medium was replaced by CCK-8 for 2.5 hours, avoiding light, at 37°C and then replaced by DMEM. After removal of the medium, absorbance (A) of cells was measured, at 450 nm, with a microplate reader (Tecan, Männedorf, Switzerland). Three independent experiments were performed in quadruplicate wells. The inhibition rate (P) was calculated as follows:

$$P = \frac{1 - A \text{ in treated cells}}{A \text{ in control cells}} \times 100\% \quad (1)$$

At last, the 50% inhibitory concentration (IC_{50}) for each of the three experimental groups was obtained.

Cell apoptosis assay

Apoptosis in the three experimental groups was measured using an Annexin V-PE/7-AAD (7-amino-actinomycin D) apoptosis detection kit (Kaiji Biology, Nanjing, People's Republic of China). Briefly, cells incubated with TMZ (4 μg/mL) for 120 hours from the CCK-8 experiment were cultured in 6 cm dishes, then trypsinized, washed, and incubated with 7-AAD staining solution under darkness. The cell suspension was then mixed with Annexin V-PE antibody under darkness for 15 minutes at RT and then, analyzed by flow cytometry (FACSCalibur; BD Biosciences, Franklin Lakes, NJ, USA).

Intraperitoneal human glioblastoma xenograft model

For the study, 40 nude mice were used. All animals were housed in a specific pathogen-free environment prior to the experiment, with free access to food and water in a temperature- and humidity-controlled room (26°C–28°C and 40% humidity) under a 10-hour light/14-hour dark cycle.

Table 1 List of gene-specific primers, expected product sizes for qRT-PCR

Gene	Primer sequences	Product size (bp)
AKT2	F 5′-CAGACGAGAGGGAGGAGTGGATG-3′	70
	R 5′-CTGGGGGAGCCACACTTGTAGTC-3′	
Bcl-2	F 5′-CCCTGTGGATGACTGAGTACCTG-3′	89
	R 5′-GCCGTACAGTTCCACAAAGGC-3′	
Caspase-3	F 5′-TCATTATTCAGGCCTGCCGTGGTA-3′	178
	R 5′-TGGATGAACCAGGAGCCATCCTTT-3′	
MDR1	F 5′-TTGGACACAGAAAGCGAAGCAG-3′	107
	R 5′-TCAGCATTACGAACTGTAGACAAACG-3′	
MRP1	F 5′-GCCTGTTTTGGTAAAGAACTGGAAG-3′	110
	R 5′-CCTTGGAACTCTCTTTCGGCTG-3′	
MGMT	F 5′-TCTTCACCATCCCGTTTTCCAG-3′	83
	R 5′-CTTCTCCGAATTTCACAACCTTCAG-3′	
GAPDH	F 5′-CATGAGAAGTATGACAACAGCCT-3′	113
	R 5′-AGTCCTTCCACGATACCAAAGT-3′	

Abbreviation: qRT-PCR, quantitative reverse-transcription polymerase chain reaction.

Glioblastoma tumors were established by intraperitoneal injection of approximately 2×10^6 human U251 cells in 200 µL suspension. Palpable tumors developed within 10–15 days. On the 20th day after implantation, 24 mice with obvious tumors were selected and randomly assigned to one of four groups (n=6): saline group (blank), TMZ treatment, TMZ plus Lenti-GFP (negative control), and TMZ plus AKT2-shRNA. Animals were given 300 µL every 3 days, for totally 16 days. Highlighted text could be changed to every 3 days for totally 16 days. Mice were euthanized 6 days after treatment withdrawal. The tumors were dissected and frozen rapidly for transcriptional analysis (PCR) or were fixed followed by embedding, for morphological and immunohistological analysis. Tumor volumes, growth rate, and inhibition rate were calculated based on the formulas:

$$\text{Volume} = 0.5263\times \text{length} \times \text{width} \times \text{thickness mm}^3 \quad (2)$$

$$\text{Growth rate} = \frac{\text{Final volume} - \text{initial volume}}{\text{Initial volume}} \quad (3)$$

and

$$\text{Inhibition rate} = \frac{\text{Tumor mass of blank control} - \text{tumor mass of treatment}}{\text{Tumor mass of blank control}} \quad (4)$$

Tissue collection and immunohistological analysis

Formalin-fixed, paraffin-embedded tumor tissues were sectioned with a vibratome. Then, 8 µm tissue sections were deparaffinized in xylene and rehydrated in a graded ethanol series. Endogenous peroxidase activity was quenched by 20-minute incubation in a 3% hydrogen peroxide solution. Thereafter, antigen retrieval was performed in prewarmed citric acid buffer (95°C, pH 6.0) for 20 minutes plus microwave heating for 5 minutes. The sections were incubated in goat serum at RT for 10 minutes to block non-specific antibody bindings and then incubated overnight at 4°C in AKT2 primary monoclonal antibody (1:100; Abgent). After washing with phosphate-buffered saline (PBS), the immunolabeled sections were incubated with peroxidase-conjugated secondary antibody (1:2,000; Jackson ImmunoResearch Laboratories Inc.) for 30 minutes at RT and finally visualized with 3,3′-diaminobenzidinand (KangWei Century, People's Republic of China) and counterstained with hematoxylin. To ensure the specificity of the immunostaining, negative controls were prepared by replacing the primary antibody with nonimmune serum. The positive-*AKT2* cells were expressed as the calculation of positively stained cells/entire malignant cell population.

In situ detection of apoptosis

The presence of apoptotic glioma cells in the four groups was measured by means of an in situ labeling of DNA fragmentation (terminal deoxynucleotidyl transferase dUTP nick end labeling [TUNEL] test kit [Kaiji, Shanghai, People's Republic of China]). In brief, from the same tumor samples previously fixed for immunohistochemical staining, 8 µm sections were obtained by vibratome. After deparaffinization and rehydration, tissue sections were permeated with 2% Proteinase K working solution, and then the TUNEL kit was applied, according to manufacturer's instruction. After the sections were washed with PBS, they were counterstained with 4′,6-diamidino-2′-phenylindole dihydrochloride (DAPI). The negative control sections underwent an identical preparation for double-staining, with incubation of buffer solution instead of the TUNEL reaction mixture. The positive controls were prepared by the same protocol on tissue sections previously subjected to DNase I. The apoptotic index was calculated as:

$$\text{Apoptotic index} = \frac{\text{TUNEL} - \text{positive cells}}{\text{Entire DAPI-stained cells}} \quad (5)$$

Statistics

Data analysis was performed using SPSS software (Version 17; SPSS Inc., Chicago IL, USA). The alpha level for Type I error was set at 0.05 for rejecting null hypotheses. Descriptive data were expressed as mean ± standard deviation (SD). Data for all three glioblastoma cell groups as well as the four in vivo experiment groups were analyzed with one-way analysis of variance (ANOVA), followed by Dunnett's *t*-test to compare the values between two groups. Immunoblot bands were visualized and quantified by ImageJ software (NIH, Bethesda, ND, USA). *P*-value less than 0.05 was considered as significant.

Results

AKT2-shRNA decreased expression level of *AKT2* in the human glioma cell line U251

After transfection, qRT-PCR analysis for *AKT2* expression demonstrated a 68% decrease in U251 glioblastoma cells stably transfected with AKT2-shRNA compared with the untransfected parental control cultures (Figure 1A). Western blot analysis confirmed the decrease in AKT2 protein expression, which was reduced by 72.9% in the

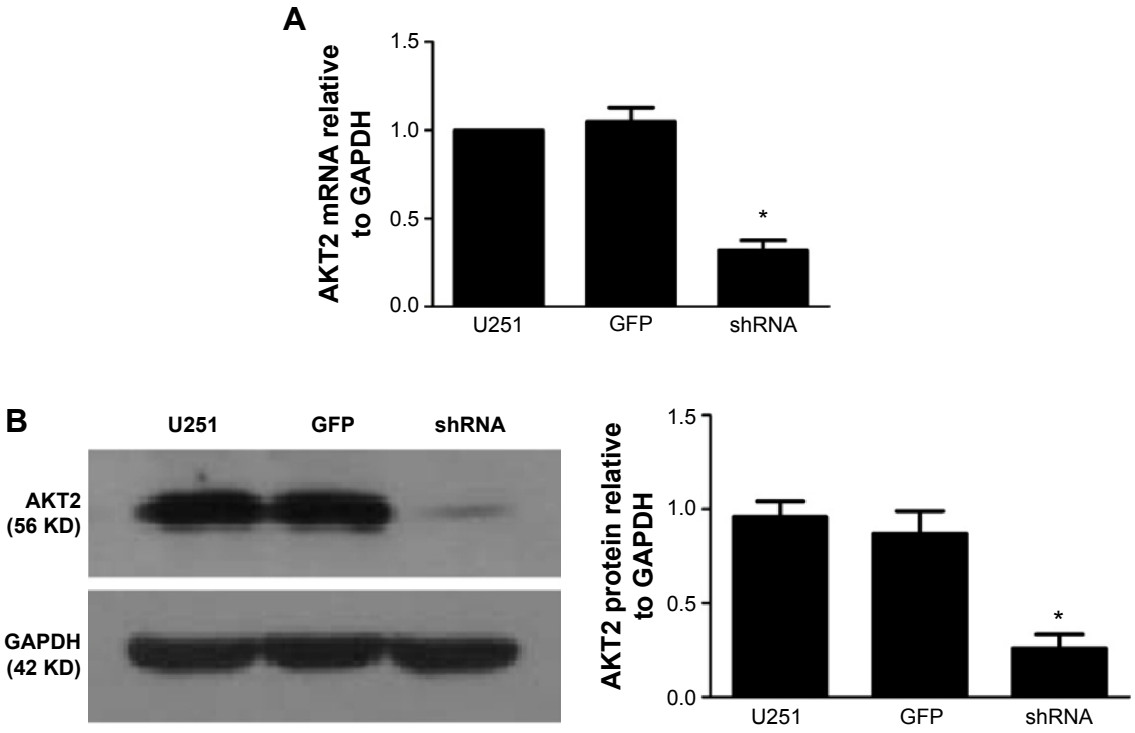

Figure 1 Effects of AKT2-shRNA transfection on *AKT2* expression.
Notes: (**A**) qRT-PCR analysis demonstrates that *AKT2* mRNA was significantly suppressed in AKT2-shRNA transfected cells compared with untransfected U251 cells and cells stably transfected with Lenti-GFP. (**B**) Western blot analysis revealed reduced AKT2 protein in U251 cells transfected with the *AKT2*-targeted shRNA compared with GFP-transfected and control U251 cells. Data are representative of three independent experiments. *$P<0.01$ as compared with control groups.
Abbreviations: GFP, green fluorescent protein; Lenti-GFP, vectors-including control shRNA and GFP sequence; mRNA, messenger RNA; qRT-PCR, quantitative reverse-transcription polymerase chain reaction; shRNA, short hairpin RNA.

AKT2-shRNA-transfected U251 (Figure 1B). In contrast, *AKT2* messenger RNA (mRNA) and protein levels were almost unchanged (105% and 90.6% of control respectively) in cells transfected with the Lenti-GFP vector.

AKT2-knockdown increased cell chemosensitivity and enhanced apoptosis in TMZ-treated U251 cells

Incubation with TMZ resulted in a inhibition of cell viability, as indicated by daily CCK-8 assays. After incubation with incremental TMZ concentrations, all three experimental cultures showed decreased cell viability, with a more significant decrease of survival rate showed in the AKT2-shRNA cell line (Figure 2A). We evaluated the chemosensitivity of each cell line by means of IC_{50}. We found that the AKT2-shRNA cells had a much lower IC_{50} (27.23±1.93 μg/mL) than that of the Lenti-GFP cells and untreated cells (39.43±2.24 μg/mL and 39.72±2.41 μg/mL, respectively) (Figure 2A).

The rate of cellular apoptosis in these three experimental cell lines was examined after 120 hours of incubation with TMZ, by flow cytometric analysis with Annexin V/7-AAD double staining. The cellular apoptosis rate of the U251 cells was 38.16%±4.83% in the AKT2-shRNA transfectants, 17.93%±2.29% in the Lenti-GFP transfectants, and 16.95%±1.32% in the untransfected controls (Figure 2B).

Knockdown of *AKT2* reduces tumor size and increases apoptosis in vivo

To examine whether altered *AKT2* expression can affect the tumor growth and survival of glioma cells treated with TMZ, we implanted U251 glioma cells intraperitoneally in nude mice to establish a xenograft model. To better mimic the future clinical modality, the tumor-implanted animals were given four different treatments. We found that the TMZ plus AKT2-shRNA-treated mice demonstrated smaller tumor size and higher inhibition rate (relative tumor volume with respect to the saline group) than did the TMZ plus Lenti-GFP-, TMZ-alone, and saline-treated mice (58.14%, 44.67%, and 41.72% respectively). These results are shown in Table 2 and Figure 3A.

We then examined in vivo apoptosis of the xenograft, using TUNEL staining. Conversely with tumor size, the tumor cells receiving TMZ plus AKT2-shRNA displayed an obviously higher percentage of TUNEL-stained (apoptotic)

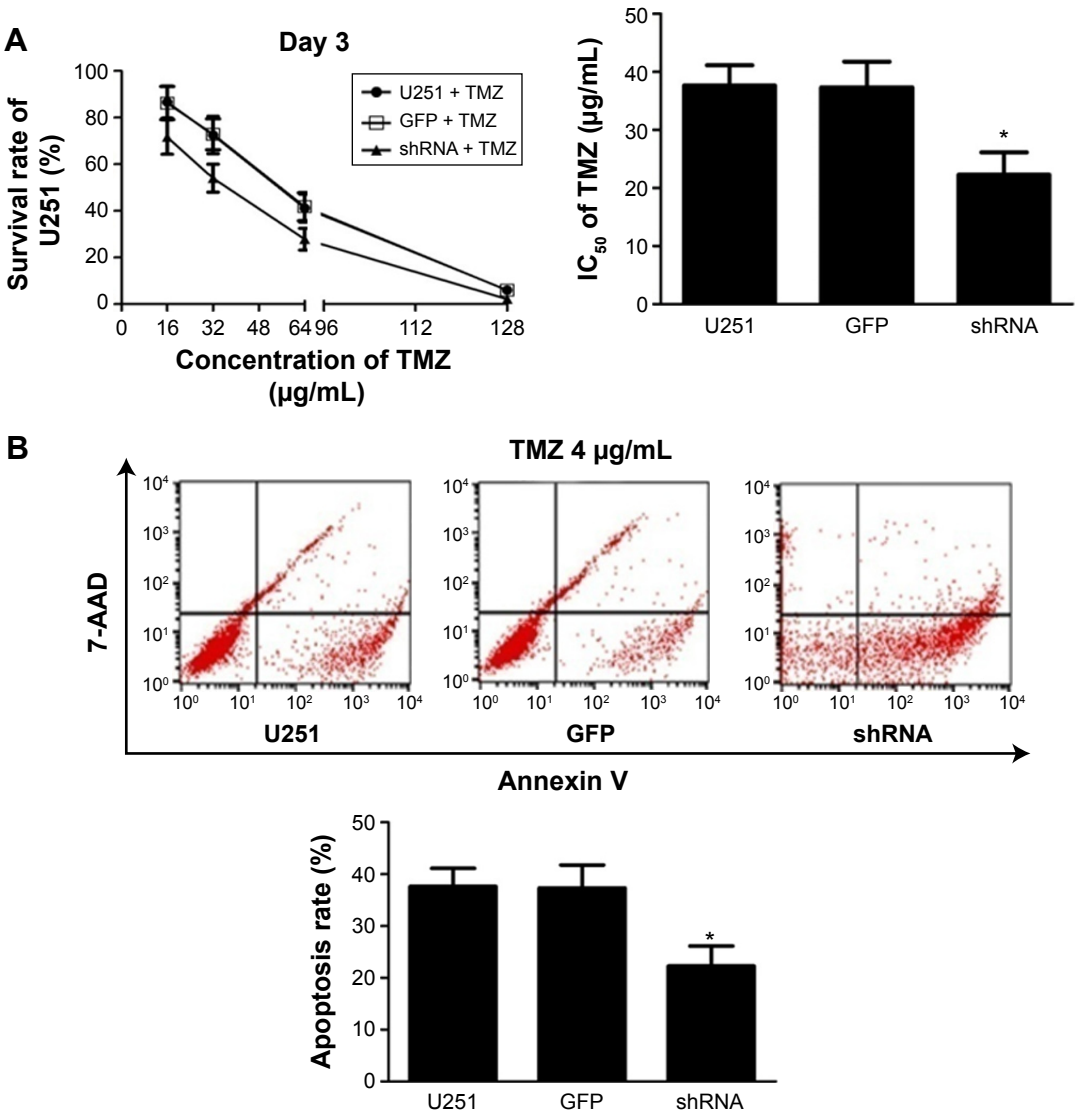

Figure 2 Effect of *AKT2* interference on cell chemosensitivity and apoptosis in TMZ-treated U251 cells.
Notes: (**A**) Left: Concentration-dependent growth inhibitory effects in all groups, with decreased survival rate in the AKT2-shRNA-transfected cells. Right: The IC_{50} value for TMZ in AKT2-shRNA-transfected U251 cells was significantly lower than that in the nontransfected and Lenti-GFP-transfected cultures, indicative of higher TMZ-sensitivity in U251 cells underexpressing *AKT2*. (**B**) Apoptosis rate was measured in Annexin V-stained cells by flow cytometry. Apoptotic cell numbers were significantly higher in the cells transfected with the AKT2-shRNA compared with the GFP-transfected and control U251 cell cultures. *$P<0.05$ vs control groups.
Abbreviations: GFP, green fluorescent protein; Lenti-GFP, vectors-including control shRNA and GFP sequence; TMZ, temozolomide; IC_{50}, 50% inhibitory concentration; shRNA, short hairpin RNA; 7-AAD, 7-amino-actinomycin D.

cells compared with the tumor cells undergoing the other three treatments (Figure 3B). Thus, the suppression of AKT2-shRNA interfered with tumor viability and was associated with increased apoptosis.

Expression of *AKT2* in tumor samples was inhibited by AKT2-shRNA intervention

To confirm that the tumor inhibition and increased apoptosis are correlated with *AKT2* expression, we performed immunohistochemical staining of AKT2 in the implanted U251 glioma samples. Tumors injected with TMZ plus AKT2-shRNA exhibited an obvious decrease in AKT2-positive cells compared with tumors injected with TMZ plus Lenti-GFP, TMZ alone, and saline. Accordingly, qRT-PCR further demonstrated similar results to those for in situ protein expression (Figure 3C).

AKT2-knockdown affected apoptosis, DNA repair, and drug efflux pump-related proteins at transcriptional and expressional levels

After having observed increased chemosensitivity and enhanced apoptosis caused by *AKT2*-knockdown, both

Table 2 Profiles of implanted tumor growth, inhibition rate, and apoptosis index

Groups	Tumor mass (g)	Tumor volume (mm^3)	Inhibition rate (%)	Apoptosis index (%)
Saline	1.25±0.26	669.34±98.73		7.15±1.04
TMZ	0.72±0.11	399.86±55.26	41.72±0.71	25.26±2.71
TMZ + GFP	0.69±0.07	383.81±34.01	44.67±2.82	26.63±3.46
TMZ + AKT2-shRNA	0.52±0.07*	297.72±41.49*	58.14±3.13	42.81±5.97*

Notes: Growth was indicated by the mass and volume. The inhibition rate was calculated as the volume of saline group subtracting each other group over saline group. The apoptosis index was calculated as the number of TUNEL-positive cells over total DAPI-stained cells. *$P<0.05$ vs control groups.

Abbreviations: DAPI, 4′,6-diamidino-2′-phenylindole dihydrochloride; GFP, green fluorescent protein; TUNEL, terminal deoxynucleotidyl transferase dUTP nick end labeling; shRNA, short hairpin RNA; TMZ, temozolomide.

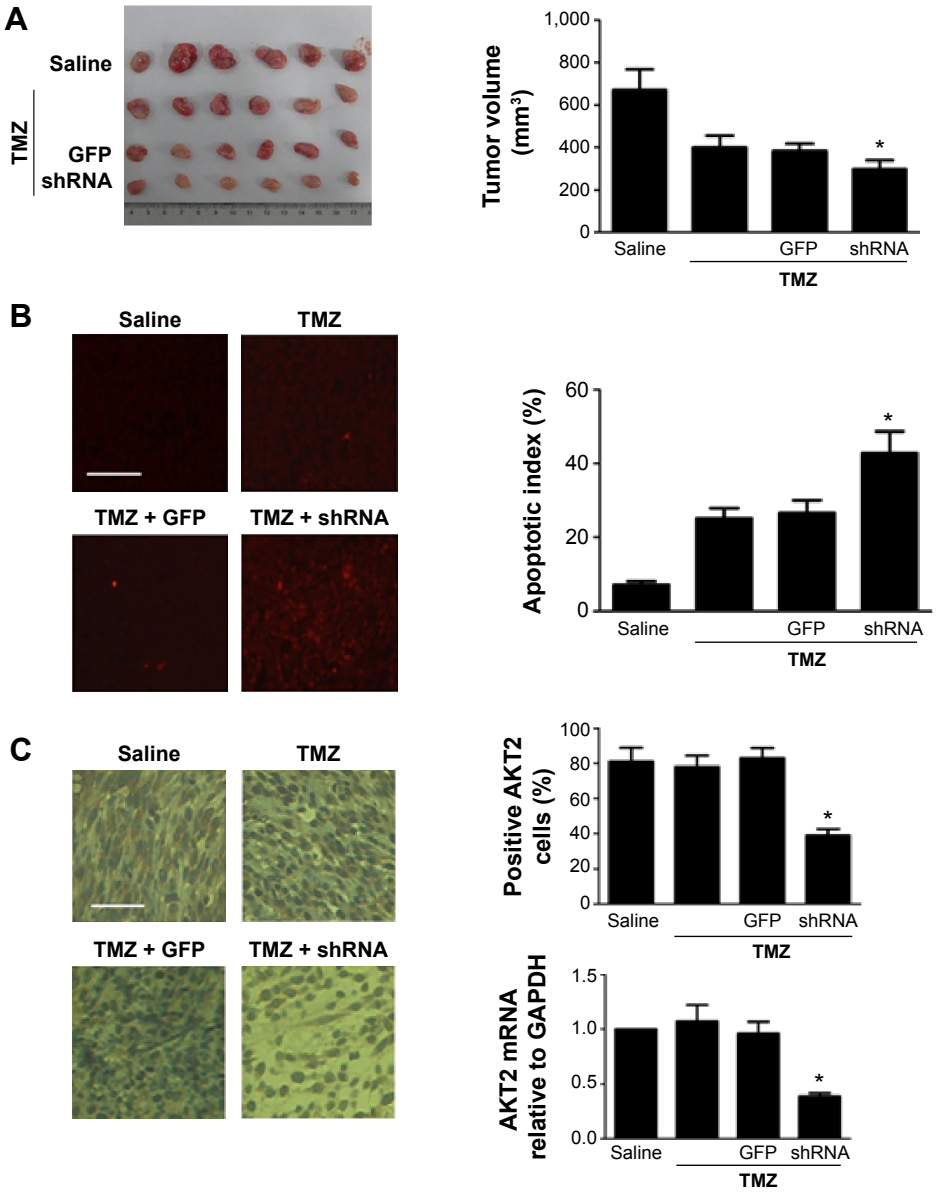

Figure 3 Effects of *AKT2*-inhibition on both tumor viability in TMZ therapy and *AKT2* expression in nude mice.

Notes: (**A**) Growth of implanted tumor cells was monitored by tumor volume. *AKT2*-targeted shRNA together with TMZ significantly suppressed the growth rate (tumor volume) in mice compared with the TMZ plus Lenti-GFP, and TMZ-alone groups. (**B**) Tumors receiving TMZ plus AKT2-shRNA showed an obviously higher percentage of apoptosis by analysis of TUNEL staining. (**C**) Immunohistochemistry and qRT-PCR analysis showed significant decrease of in situ expression of *AKT2* in TMZ plus shRNA-treated mice. *$P<0.05$ vs saline group. Bar =100 μm.

Abbreviations: GFP, green fluorescent protein; Lenti-GFP, vectors-including control shRNA and GFP sequence; mRNA, messenger RNA; qRT-PCR, quantitative reverse-transcription polymerase chain reaction; shRNA, short hairpin RNA; TMZ, temozolomide; TUNEL, terminal deoxynucleotidyl transferase dUTP nick end labeling.

in vitro and vivo, we examined the transcription and expression level of the antiapoptotic protein Bcl-2 and apoptosis effector caspase-3 in the different TMZ-treated glioblastoma transfectants. As shown in Figure 4A and B, mRNA and protein levels of Bcl-2 were significantly lower in the AKT2-shRNA transfectants compared with the control cells, whereas caspase-3 expression was significantly higher than in the control groups. Then, we surmised that the increased sensitivity to TMZ could be due to other contributors, such as DNA repair protein MGMT, and drug transporter proteins MDR1 and MRP1. The results showed significant decreased protein expressions and mRNA levels of MRP1 and MGMT proteins in the AKT2-shRNA-transfected cells. However, the mRNA and protein levels of MDR1 remained unchanged among the three cell lines (Figure 4A and B).

Discussion

In this study, we provide compelling evidence that in human glioblastoma cell line U251, the underexpression of *AKT2* caused by shRNA transfection promoted apoptosis, inhibited cell viability, and enhanced cell sensitivity to TMZ, both in vitro and in vivo. shRNA-mediated knockdown of *AKT2* also altered the expression of several chemoresistance-related genes in U251 cells. These findings are in agreement with our previous work with the U87 cell line, demonstrating that *AKT2* performs multiple functions as an oncogene, with the key characteristics of presenting chemoresistance in glioma.

As chemoresistance is the primary obstacle for glioma patients undergoing standard chemoradiotherapy after surgical dissection of tumor, and *AKT2* is found to be significantly overexpressed in glioblastoma patients with shorter survival duration (8 months with overexpressed AKT2 vs 18 months without AKT2 overexpression) receiving the same chemotherapy,[12] we hereby evaluated the effect of *AKT2* on tumor viability and chemoresistance, using the currently mostly applied alkylating agent, TMZ. As expected, *AKT2* expression change obviously affected the response of tumor cells to TMZ treatment: In vitro, the IC_{50} of U251 glioma

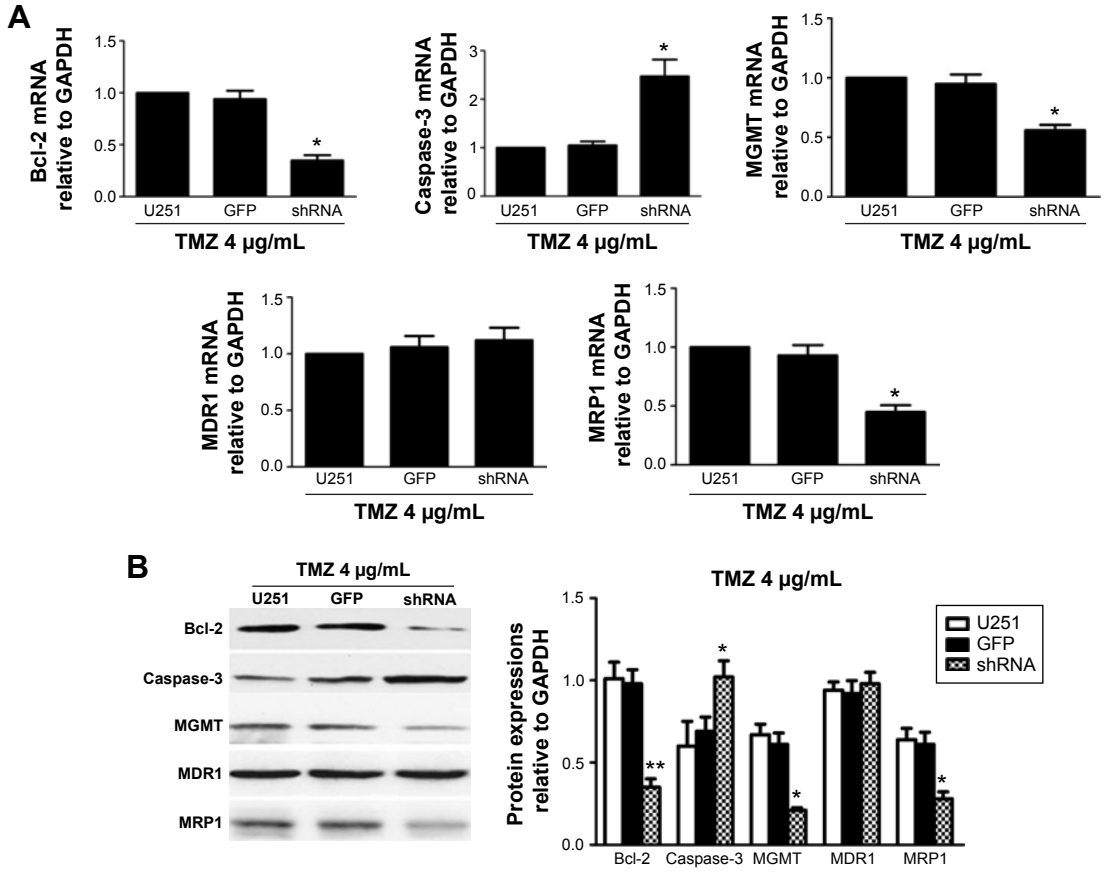

Figure 4 mRNA and protein alterations related to U251 cell chemoresistance by AKT2 inhibition.
Notes: (**A**) *AKT2*-targeted shRNA altered MRP1, MGMT, Bcl-2, and caspase-3 mRNA transcription in U251 cells in the presence of 4 μg/mL TMZ. There was a decrease in antiapoptotic Bcl-2, DNA repairing MGMT, and drug pump MRP1 mRNA, and an increase in apoptotic effector caspase-3 mRNA. (**B**) Western-blots revealed similar relationship with *AKT2*-knockdown, where caspase-3 proteins were significantly higher, while MGMT, MRP1, and Bcl-2 proteins were expressed at a lower level. However, there was no significant changes in the mRNA and protein levels of MDR1. *$P<0.05$. **$P<0.01$ vs control groups.
Abbreviations: GFP, green fluorescent protein; mRNA, messenger RNA; shRNA, short hairpin RNA; TMZ, temozolomide.

cells was much lower after knockdown of *AKT2* RNA in the AKT2-shRNA transfected; in vivo, the tumor volume and tumor mass were significantly inhibited in the AKT2-shRNA and TMZ combined-treatment mice.

The potential mechanism of tumor chemoresistance could be complicated. Most of the traditional glioma chemotherapy agents act on tumor cells by inducing cell DNA damage, which can in turn, induce cell apoptosis. Correspondingly, glioma cells can encounter the apoptotic effect through inhibitory regulations of apoptosis pathway.[17] In this study, we observed, in both in vitro experiments and tumor-implanted mice, that this antiapoptotic effect was reversed by *AKT2*-knockdown. Moreover, we investigated the relation between the *AKT2* gene and apoptosis, by means of protein and enzymatic analysis, to address the molecular mechanisms of this shRNA-mediated apoptosis. We analyzed oncogene *Bcl-2*, which has been related to a decreased effect of irradiation and cytotoxic drugs in malignant glioma cells,[19] and main terminal cleavage enzyme caspase-3 expression, demonstrating that reduced AKT2 expression was associated with higher apoptotic effector caspase-3 expression and lower antiapoptotic Bcl-2 expression. So, *AKT2*-knockdown induced glioma cell apoptosis, not only in its natural growth,[11] but also, during chemotherapy.

On the other hand, it has been previously reported that exposure to TMZ induces cell cycle arrest, which implies that before cells go into apoptosis, the tumor cell itself may initiate specific DNA repair during this period, to reverse the TMZ-induced damage and restore their tumorous functions. TMZ methylates DNA purine residues, especially O6-guanine, in brain tumors (which favor prodrug activation by possessing a more alkaline pH than surrounding healthy tissue), thereby creating O6-methyl-guanine lesions, which are largely responsible for TMZ cytotoxicity.[18] DNA repair protein MGMT stoichiometrically and rapidly removes the methyl groups from O6-methylguanine, therefore leading to TMZ-resistance in patients, resulting in treatment failure. In the present study, analysis of MGMT revealed *AKT2*-suppression decreased *MGMT* expression at both mRNA and protein levels, which strongly supported that glioblastoma cells partly present resistance to TMZ toxicity by promptly repairing their DNA lesions through the *AKT2* gene pathway. However, even the *MGMT* gene is silenced or deactivated, by promoter methylation for example, the glioblastoma could also confer chemoresistance in many clinical cases, where patients, at last, suffer from tumor recurrence or progress. This phenomenon indicates other molecular mechanisms participate in the repair pathway of nucleic acid. The previously studied and known molecular processes include mismatch repair (MMR), base excision repair (BER), and nucleotide excision repair (NER), which need to be deeply explored in future studies.[17,20]

Furthermore, another important mechanism that affects chemotherapeutic outcomes is the presence of drug transporters, such as the overexpression of the ABC superfamily. MDR1 and MRP1 represent members of the ABC superfamily of transmembrane proteins, the expression level of which were reported to increase in cells derived from high-grade glioblastomas compared with low-grade astrocytomas. Moreover, MRP1 has previously been shown to be expressed on the membrane of vascular endothelial cells in some high-grade gliomas, implying that it may limit the intake of cytotoxic drugs and prevent such drugs from reaching a concentration that can kill cells.[21] Our study of the relationship between *AKT2* and drug transporters showed decreased MRP1, in both transcriptional and expressional protein levels, in *AKT2*-knockdown cells. This result is consistent with the finding in our VM-26-treated U87 cells, demonstrating that MRP1, instead of MDR1, is involved in *AKT2*-mediated chemoresistance.

However, our current study here is not likely to cover the complete mechanisms of chemoresistance in glioblastoma, as MDR could be either intrinsic resistance (at the beginning of chemotherapy) or acquired resistance (acquired over the period of treatment), and the latter is more attributed to genetic mutations and the selection of the therapy.[16] This will be further studied using TMZ-resistant cell lines, with our high-throughput protein chip.

Conclusion

In summary, the downregulation of AKT2 enhanced apoptosis and suppressed the viability of glioblastoma cells in vitro; meanwhile AKT2-targeted therapy combined with TMZ inhibited tumor growth in vivo. Furthermore, the chemoresistance-related study showed *AKT2* gene-knockdown in glioblastoma cells in the presence of 4 μg/mL TMZ decreased Bcl-2 and increased caspase-3 in the apoptosis pathway, decreased MGMT in the DNA repair system, and then decreased the drug transporter of MRP1. The results of this study, together with our previous findings in VM-26-treated U87 cells, identify AKT2 as an ideal prognostic marker and an attractive therapeutic target for overcoming chemoresistance, which will eventually lead to the success of glioblastoma treatment.

Acknowledgment

This work was supported by the National Natural Sciences Fund Project of China (grant number 30930094).

Disclosure

The authors report no conflicts of interest in this work.

References

1. Bleeker FE, Molenaar RJ, Leenstra S. Recent advances in the molecular understanding of glioblastoma. *J Neurooncol*. 2012;108(1):11–27.
2. Van Meir EG, Hadjipanayis CG, Norden AD, Shu HK, Wen PY, Olson JJ. Exciting new advances in neuro-oncology: the avenue to a cure for malignant glioma. *CA Cancer J Clin*. 2010;60(3):166–193.
3. Toker A, Yoeli-Lerner M. Akt signaling and cancer: surviving but not moving on. *Cancer Res*. 2006;66(8):3963–3966.
4. Mueller S, Phillips J, Onar-Thomas A, et al. PTEN promoter methylation and activation of the PI3K/Akt/mTOR pathway in pediatric gliomas and influence on clinical outcome. *Neuro Oncol*. 2012;14(9):1146–1152.
5. Bellacosa A, de Feo D, Godwin AK, et al. Molecular alterations of the AKT2 oncogene in ovarian and breast carcinomas. *Int J Cancer*. 1995;64(4):280–285.
6. Cheng JQ, Godwin AK, Bellacosa A, et al. AKT2, a putative oncogene encoding a member of a subfamily of protein-serine/threonine kinases, is amplified in human ovarian carcinomas. *Proc Natl Acad Sci U S A*. 1992;89(19):9267–9271.
7. Cheng JQ, Ruggeri B, Klein WM, et al. Amplification of AKT2 in human pancreatic cells and inhibition of AKT2 expression and tumorigenicity by antisense RNA. *Proc Natl Acad Sci U S A*. 1996;93(8):3636–3641.
8. Liao Y, Grobholz R, Abel U, et al. Increase of AKT/PKB expression correlates with gleason pattern in human prostate cancer. *Int J Cancer*. 2003;107(4):676–680.
9. Ringel MD, Hayre N, Saito J, et al. Overexpression and overactivation of Akt in thyroid carcinoma. *Cancer Res*. 2001;61(16):6105–6111.
10. Nakayama H, Ikebe T, Beppu M, Shirasuna K. High expression levels of nuclear factor kappaB, IkappaB kinase alpha and Akt kinase in squamous cell carcinoma of the oral cavity. *Cancer*. 2001;92(12):3037–3044.
11. Cui Y, Wang Q, Wang J, et al. Knockdown of AKT2 expression by RNA interference inhibits proliferation, enhances apoptosis, and increases chemosensitivity to the anticancer drug VM-26 in U87 glioma cells. *Brain Res*. 2012;1469:1–9.
12. Zhao Z, Liu Y, He H, Chen X, Chen J, Lu YC. Candidate genes influencing sensitivity and resistance of human glioblastoma to Semustine. *Brain Res Bull*. 2011;86(3–4):189–194.
13. Newlands ES, O'Reilly SM, Glaser MG, et al. The Charing Cross Hospital experience with temozolomide in patients with gliomas. *Eur J Cancer*. 1996;32A(13):2236–2241.
14. Stupp R, Mason WP, van den Bent MJ, et al; European Organisation for Research and Treatment of Cancer Brain Tumor and Radiotherapy Groups; National Cancer Institute of Canada Clinical Trials Group. Radiotherapy plus concomitant and adjuvant temozolomide for glioblastoma. *N Engl J Med*. 2005;352(10):987–996.
15. Bredel M. Anticancer drug resistance in primary human brain tumors. *Brain Res Rev*. 2001;35(2):161–204.
16. Lu C, Shervington A. Chemoresistance in gliomas. *Mol Cell Biochem*. 2008;312(1–2):71–80.
17. Happold C, Roth P, Wick W, et al. Distinct molecular mechanisms of acquired resistance to temozolomide in glioblastoma cells. *J Neurochem*. 2012;122(2):444–455.
18. Zhang J, Stevens MF, Laughton CA, Madhusudan S, Bradshaw TD. Acquired resistance to temozolomide in glioma cell lines: molecular mechanisms and potential translational applications. *Oncology*. 2010;78(2):103–114.
19. Weller M, Malipiero U, Aguzzi A, Reed JC, Fontana A. Protooncogene bcl-2 gene transfer abrogates Fas/APO-1 antibody-mediated apoptosis of human malignant glioma cells and confers resistance to chemotherapeutic drugs and therapeutic irradiation. *J Clin Invest*. 1995;95(6):2633–2643.
20. Auger N, Thillet J, Wanherdrick K, et al. Genetic alterations associated with acquired temozolomide resistance in SNB-19, a human glioma cell line. *Mol Cancer Ther*. 2006;5(9):2182–2192.
21. Spiegl-Kreinecker S, Buchroithner J, Elbling L, et al. Expression and functional activity of the ABC-transporter proteins P-glycoprotein and multidrug-resistance protein 1 in human brain tumor cells and astrocytes. *J Neurooncol*. 2002;57(1):27–36.